frontiers in Physiology

ORIGINAL RESEARCH
published: 14 May 2021
doi: 10.3389/fphys.2021.642986

Development of a Novel Web Camera-Based Contact-Free Major Depressive Disorder Screening System Using Autonomic Nervous Responses Induced by a Mental Task and Its Clinical Application

*Batbayar Unursaikhan[1,2], Nobuaki Tanaka[3], Guanghao Sun[4], Sadao Watanabe[5], Masako Yoshii[6], Kazuki Funahashi[6], Fumihiro Sekimoto[4], Fumiaki Hayashibara[1], Yutaka Yoshizawa[1], Lodoiravsal Choimaa[2] and Takemi Matsui[1]**

[1] Graduate School of System Design, Tokyo Metropolitan University, Tokyo, Japan, [2] Machine Intelligence Laboratory, School of Engineering and Applied Sciences, National University of Mongolia, Ulaanbaatar, Mongolia, [3] BESLI Clinic, Tokyo, Japan, [4] Graduate School of Informatics and Engineering, The University of Electro-Communications, Tokyo, Japan, [5] Vital Lab, Ltd., Tokyo, Japan, [6] RICOH Company, Ltd., Tokyo, Japan

OPEN ACCESS

Edited by:
Ahsan H. Khandoker,
Khalifa University,
United Arab Emirates

Reviewed by:
Bhavesh Patel,
California Medical Innovations Institute, United States
Clarissa Lim Velayo,
University of the Philippines Manila, Philippines

***Correspondence:**
Takemi Matsui
tmatsui@tmu.ac.jp

Specialty section:
This article was submitted to Computational Physiology and Medicine, a section of the journal Frontiers in Physiology

Received: 04 February 2021
Accepted: 23 April 2021
Published: 14 May 2021

Citation:
Unursaikhan B, Tanaka N, Sun G, Watanabe S, Yoshii M, Funahashi K, Sekimoto F, Hayashibara F, Yoshizawa Y, Choimaa L and Matsui T (2021) Development of a Novel Web Camera-Based Contact-Free Major Depressive Disorder Screening System Using Autonomic Nervous Responses Induced by a Mental Task and Its Clinical Application. Front. Physiol. 12:642986. doi: 10.3389/fphys.2021.642986

Background: To increase the consultation rate of potential major depressive disorder (MDD) patients, we developed a contact-type fingertip photoplethysmography-based MDD screening system. With the outbreak of SARS-CoV-2, we developed an alternative to contact-type fingertip photoplethysmography: a novel web camera-based contact-free MDD screening system (WCF-MSS) for non-contact measurement of autonomic transient responses induced by a mental task.

Methods: The WCF-MSS measures time-series interbeat intervals (IBI) by monitoring color tone changes in the facial region of interest induced by arterial pulsation using a web camera (1920 × 1080 pixels, 30 frames/s). Artifacts caused by body movements and head shakes are reduced. The WCF-MSS evaluates autonomic nervous activation from time-series IBI by calculating LF (0.04–0.15 Hz) components of heart rate variability (HRV) corresponding to sympathetic and parasympathetic nervous activity and HF (0.15–0.4 Hz) components equivalent to parasympathetic activities. The clinical test procedure comprises a pre-rest period (Pre-R; 140 s), mental task period (MT; 100 s), and post-rest period (Post-R; 120 s). The WCF-MSS uses logistic regression analysis to discriminate MDD patients from healthy volunteers via an optimal combination of four explanatory variables determined by a minimum redundancy maximum relevance algorithm: HF during MT (HF_{MT}), the percentage change of LF from pre-rest to MT ($\%\Delta LF_{(Pre-R \Rightarrow MT)}$), the percentage change of HF from pre-rest to MT ($\%\Delta HF_{(Pre-R \Rightarrow MT)}$), and the percentage change of HF from MT to post-rest ($\%\Delta HF_{(MT \Rightarrow Post-R)}$). To clinically test the WCF-MSS, 26 MDD patients (16 males and 10 females, 20–58 years) were recruited from BESLI Clinic in Tokyo, and 27 healthy volunteers (15 males and 12 females, 18–60 years) were recruited from Tokyo

Metropolitan University and RICOH Company, Ltd. Electrocardiography was used to calculate HRV variables as references.

Result: The WCF-MSS achieved 73% sensitivity and 85% specificity on 5-fold cross-validation. IBI correlated significantly with IBI from reference electrocardiography ($r = 0.97$, $p < 0.0001$). Logit scores and subjective self-rating depression scale scores correlated significantly ($r = 0.43$, $p < 0.05$).

Conclusion: The WCF-MSS seems a promising contact-free MDD screening apparatus. This method enables web camera built-in smartphones to be used as MDD screening systems.

Keywords: major depressive disorder, screening, heart rate variability, non-contact, remote photoplethysmography, autonomic nervous response, mental task

INTRODUCTION

Major depressive disorder (MDD) has become one of the most serious mental health problems; globally, over 264 million people have MDD (James et al., 2018) and up to 15% of MDD patients show suicidal intent, particularly in young people (Kessler and Bromet, 2013; Whiteford et al., 2013). Indeed, the number of people who have experienced MDD during their lifetime was increased by nearly 20% for the last decade (Vos et al., 2016). Over 76% of people in developing countries and over 40% of people worldwide receive no relevant medical treatment for mental health disorders owing to lack of resources and field professionals (Wang et al., 2007). To encourage people to seek psychiatric support in the early stages of MDD, we previously developed a fingertip photoplethysmography (PPG)-based MDD screening system using stress-induced autonomic transient responses (Dagdanpurev et al., 2018).

SARS-CoV-2 infection can lead to serious symptoms such as respiratory disorders or multiple organ dysfunction (Dockery et al., 2020). SARS-CoV-2 is transmitted via oculus, nasus, and aditus facial mucosa (Yan et al., 2020), mainly through respiratory droplets and face-to-hand contact. Touching infected surfaces poses a potential risk, as people often instinctively touch their faces more than 20 times per hour (Kwok et al., 2015). Thus, we proposed a novel web camera-based contact-free MDD screening system (WCF-MSS).

Major depressive disorder is diagnosed by history taking and the criteria of the Diagnostic and Statistical Manual of Mental Disorders, Fifth Edition (DSM-5), supplemented by objective measures using biomarkers (Woods et al., 2014). Although rare, the possibility of incorrect diagnosis cannot be excluded if an examinee gives imprecise answers during history taking (Lépine et al., 1997). As an alternative to history taking, the WCF-MSS enables objective non-contact MDD screening using autonomic nervous system responses induced by a mental task (MT). Automatic nervous system activity can be evaluated using heart rate variability (HRV). The low frequency HRV component (LF: 0.04–0.15 Hz) corresponds to sympathetic and vagal tone activity and the high frequency HRV component (HF: 0.15–0.4 Hz) reflects parasympathetic activity. Previous research indicates that MDD patients have reduced HRV components at rest (Brunoni et al., 2013; Bassett, 2015; Carnevali et al., 2018). However, some researchers have reported a lack of correlation between HRV and MDD (Yeragani et al., 1991; Moser et al., 1998). These conflicting findings can be attributed to substantial individual differences in the autonomic activity of MDD patients during the rest state. Instead of using the rest state, we examined HRV-determined autonomic nervous responses induced by an MT (Sun et al., 2016). HRV is generally calculated using time-series interbeat intervals (IBI) measured by contact-based electrocardiography (ECG) or PPG. Previously, we developed HRV-based MDD screening systems using both ECG and fingertip PPG (Sun et al., 2016; Dagdanpurev et al., 2018). However, these conventional measuring techniques require contact-type sensors or electrodes. Long-term discomfort induced by contact-type devices affects the examinee's autonomic nervous system activity (Westen, 2012; Culpepper et al., 2015).

To conduct non-contact MDD screening using a web camera, we used a minimum redundancy maximum relevance (MRMR) algorithm to determine the optimal combination of HRV-related autonomic nervous activity variables. To enable non-contact monitoring of HRV, we previously developed an HRV monitoring method using Doppler radar (Suzuki et al., 2008). The use of web camera-based contact-free remote PPG (rPPG) is another non-contact method of measuring HRV. Like PPG, rPPG uses optical methodology to sense heartbeat-induced arterial volume changes (Lewandowska et al., 2011). Unlike contact-based PPG, rPPG detects blood volume pulse (BVP) by tracking changes in facial luminance induced by microscopic arterial pulsations via a remote web camera (Poh et al., 2011; Wang et al., 2017). The WCF-MSS uses rPPG instead of Doppler radar. To optimize data processing procedures specialized for rPPG, we used techniques such as multiresolution analysis of the maximum overlap discrete

Abbreviations: AUC, area under the curve; BVP, blood volume pulse; COVID-19, SARS-CoV-2; DSM-5, Diagnostic and Statistical Manual of Mental Disorders, Fifth Edition; ECG, electrocardiography; HF, high frequency; HRV, heart rate variability; IBI, interbeat intervals; LF, low frequency; LRA, logistic regression analysis; MDD, major depressive disorder; MODWTMRA, maximum overlap discrete wavelet transformation; MRMR, minimum redundancy maximum relevance; MT, mental task; NPV, negative predictive value; PPG, photoplethysmography; PPV, positive predictive value; RGB, red-green-blue; RNG, random number generation; ROC, receiver operating characteristic; ROI, region of interest; rPPG, remote photoplethysmography; SDS, Self-Rating Depression Scale; WCF-MSS, web camera-based contact-free MDD screening system.

wavelet transformation (MODWTMRA) to extract BVP from red-green-blue (RGB) color signals.

In the present study, we developed a novel WCF-MSS. Without the use of contact-type sensors or electrodes, the proposed system measures the examinee's MT-induced autonomic nervous responses via an ordinary remote web camera. All web camera built-in devices, such as smartphones, tablets, and notebooks can potentially be used at home as MDD self-screening tools without the help of healthcare professionals. The WCF-MSS seems promising as a contact-free MDD screening tool that does not spread the COVID-19 infection.

MATERIALS AND METHODS

Overview of the WCF-MSS

The WCF-MSS MDD screening procedure is shown in **Figure 1**. The proposed system uses only a web camera for HRV measurement and a display for the MT paradigm. A web camera captures moving images of the subject's face that reflect microscopic facial artery pulsations before, during, and after the MT. The system processes the captured facial images to extract heartbeat signals from facial luminance changes induced by arterial pulsations and processes the heartbeat signals to determine HRV-derived autonomic nervous activation induced by MT; this processing allows the system to differentiate MDD patients from healthy subjects. During the image-processing procedure, the system detects and tracks the subject's face to adjust the size and location of the region of interest (ROI). The facial luminance of each frame (30 frames/s) within the ROI is determined by the green signal of the web camera's RGB signals. During the signal-processing procedure, the BVP signal is determined from the green signal of the RGB signals via MODWTMRA. The LF (0.04–0.15 Hz) HRV component, the HF (0.15–0.4 Hz) HRV component, and the LF/HF are calculated using time-series IBI of the BVP signal for each measurement period; that is, the pre-rest (Pre-R), MT, and post-rest (Post-R) periods (Pre-R: 140 s, MT: 100 s, and Post-R: 120 s). Logistic regression analysis (LRA) was conducted to differentiate MDD patients from healthy volunteers via four explanatory variables related to autonomic activity.

Image Processing

Facial Detection and Tracking

We used web camera-based rPPG methods to extract the BVP signal from the pixels of the human facial skin region. To perform trace detection of exact facial skin pixels from a captured image with body movements, we developed custom image-processing software using Python programming language (Python Software Foundation)[1]. The WCF-MSS detects the facial ROI associated with luminance alteration induced by arterial pulsations using the Haar cascade classifier from the Open Computer Vision (OpenCV) library (Bradski, 2000; Lienhart and Maydt, 2002; Viola and Jones, 2004). To track the ROI when the head is moving

[1]https://www.python.org

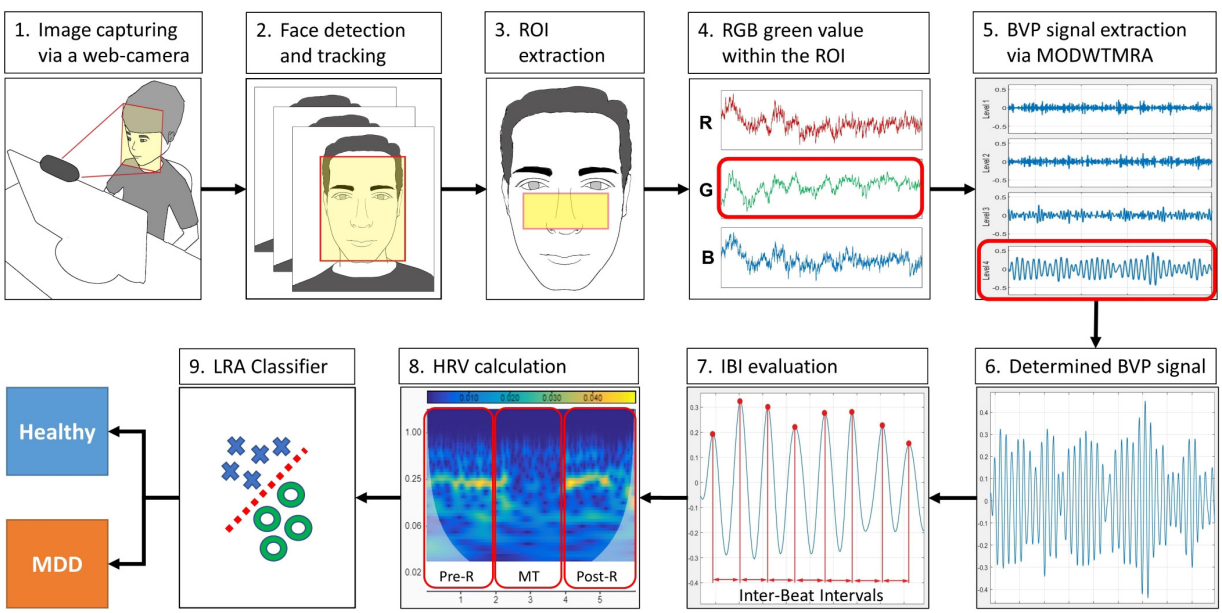

FIGURE 1 | Block diagram of the WCF-MSS MDD screening procedure. (1) Web camera-based image capture before, during, and after the mental task (MT) at 30 frames/s. (2) Facial tracking for body movement cancelation. (3) Extraction of the region of interest (ROI). (4) RGB green signal within the ROI. (5) Extraction of pulse wave using wavelet transformation (MODWTMRA). (6) Blood volume pulse (BVP) signal determined by MODWTMRA. (7) Time-series interbeat intervals evaluation. (8) Heart rate variability (HRV) calculation for autonomic nervous activation monitoring during pre-rest, random number generation (RNG) MT, and post-rest. (9) Differentiation of MDD patients from healthy volunteers using logistic regression analysis (LRA). MDD, major depressive disorder; WCF-MSS, web camera-based contact-free MDD screening system.

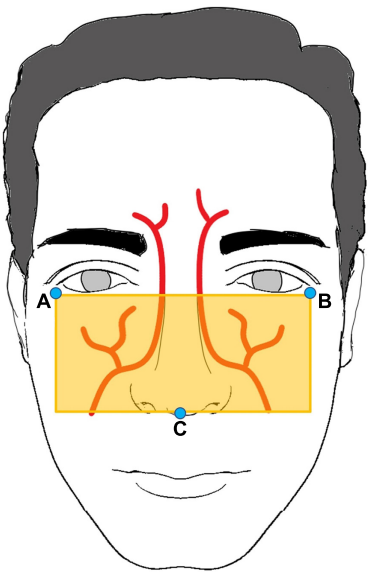

FIGURE 2 | Region of interest determined by three landmark points: A, B, and C.

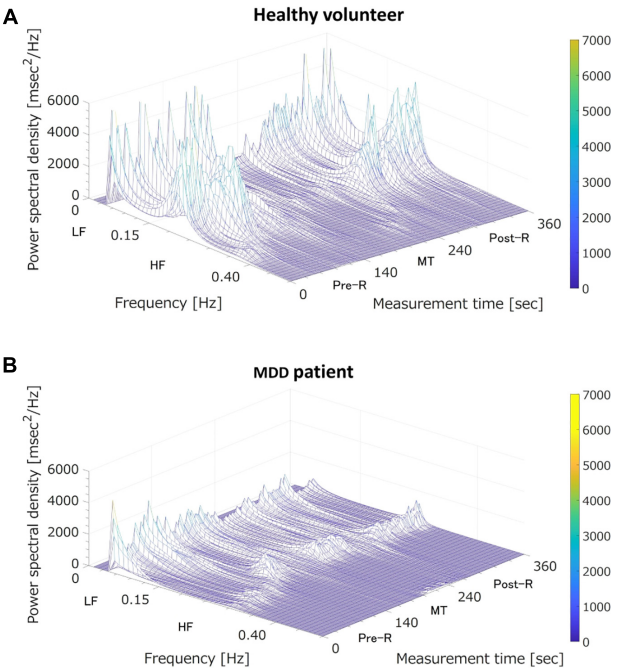

FIGURE 3 | Three-dimensional mapping of power spectral densities of heart rate variability before the mental task (MT) (Pre-R), during the MT, and after the MT (Post-R). **(A)** A healthy volunteer; MT caused a large reduction in power spectrum density in the high frequency (HF) domain (corresponding to parasympathetic nervous activation). **(B)** A major depressive disorder (MDD) patient; MT induced no specific change in power spectrum density in the HF domain (corresponding to vagal tone activation). LF, low frequency.

owing to posture-retaining balancing motions, the WCF-MSS uses the median flow object tracking algorithm (Kalal et al., 2010) from the OpenCV library. The median flow tracking algorithm keeps the ROI in the correct position during head movements.

Initializing and Adjusting the Region of Interest

To extract the BVP signal efficiently, we determined the ROI using the anatomy of the facial arteries (von Arx et al., 2018). The ROI was determined using facial landmarks (A to C), as shown in **Figure 2**. Facial landmarks were determined using the neural network-based landmark-detection algorithm from the DLIB library (King, 2009). A 0.3 s window moving average filter was used to exclude artifacts and to determine the landmark points (A to C) unaffected by head motion.

Signal Processing

Blood Volume Pulse Signal Extraction

The WCF-MSS extracts a BVP signal derived from averaged RGB green color signals within the ROI via MODWTMRA from MATLAB (The MathWorks, Inc., Natick, MA, United States). We used the MODWTMRA order 4 symlet wavelet filter with decomposition level 4 and band-pass filter (0.6–2.0 Hz), which extracts only cardiac-related signals.

Heart Rate Variability Analysis

To evaluate autonomic nervous activation induced by the MT, we used the HeartPy heart rate analysis toolkit (van Gent et al., 2018). The LF (0.04–0.15 Hz) component corresponds to HRV sympathetic and parasympathetic nervous activity and the HF (0.15–0.4 Hz) component reflects HRV parasympathetic activity. These were calculated from the time-series heartbeat intervals derived from BVP signals. LF and HF were calculated for the rest period before the MT (Pre-R), the period during the MT, and the rest period after the MT (Post-R). We determined 15 explanatory parameters for MDD classification: $LF_{(Pre-R)}$, $LF_{(MT)}$, $LF_{(Post-R)}$, $HF_{(Pre-R)}$, $HF_{(MT)}$, $HF_{(Post-R)}$, $LF/HF_{(Pre-R)}$, $LF/HF_{(MT)}$, and $LF/HF_{(Post-R)}$, their deviations between Pre-R and MT, and their deviations between MT and Post-R.

Major Depressive Disorder Screening Using Logistic Regression Analysis

To differentiate MDD patients from healthy volunteers, we used LRA from the MATLAB Machine Learning Toolbox.

TABLE 1 | The demographic of the healthy volunteers and the MDD patients.

Classifications	Number	Sex and Age		Number	Average SDS scores
Healthy	27	Sex	Male	15	34.1
			Female	12	31.7
		Age	<25	10	28.9
			25–45	14	35.5
			45>	3	35.3
MDD	26	Sex	Male	16	52.7
			Female	10	52.6
		Age	<25	4	53.5
			25–45	18	51.7
			45>	4	56.0

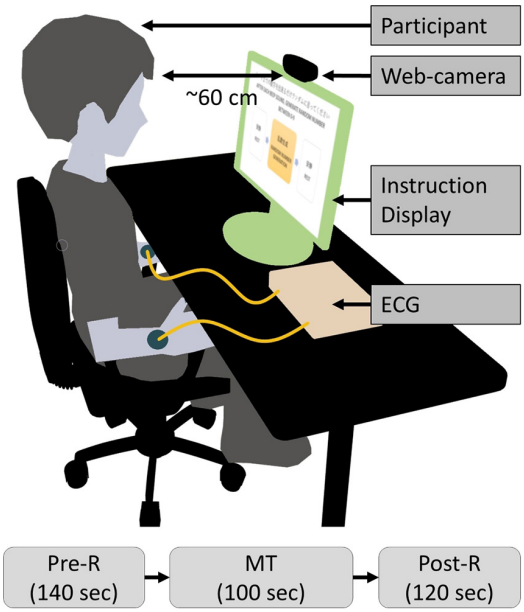

FIGURE 4 | Diagram of measurement setup and study protocol. ECG, electrocardiogram; MT, mental task.

The linear equation determined by LRA is expressed as (m = 1 to 15):

$$\log \frac{p}{1-p} = \beta_0 + \beta_1 x_1 + \beta_2 x_2 + \ldots + \beta_m x_m \quad (1)$$

Where $\log \frac{p}{1-p}$ is the predicted logit score, β_0 is a constant, and $\beta_1 \ldots \beta_m$ are regression coefficients corresponding to the LRA explanatory variables of $x_{1\ldots x}m$. In our previous study, we used the three LRA explanatory variables LF, HF, and LF/HF, corresponding to three states (i.e., before MT, during MT, and after MT). In the present study, we identified 15 explanatory variables of the classifier (Sun et al., 2016; Dagdanpurev et al., 2018) suitable for non-contact measurement:

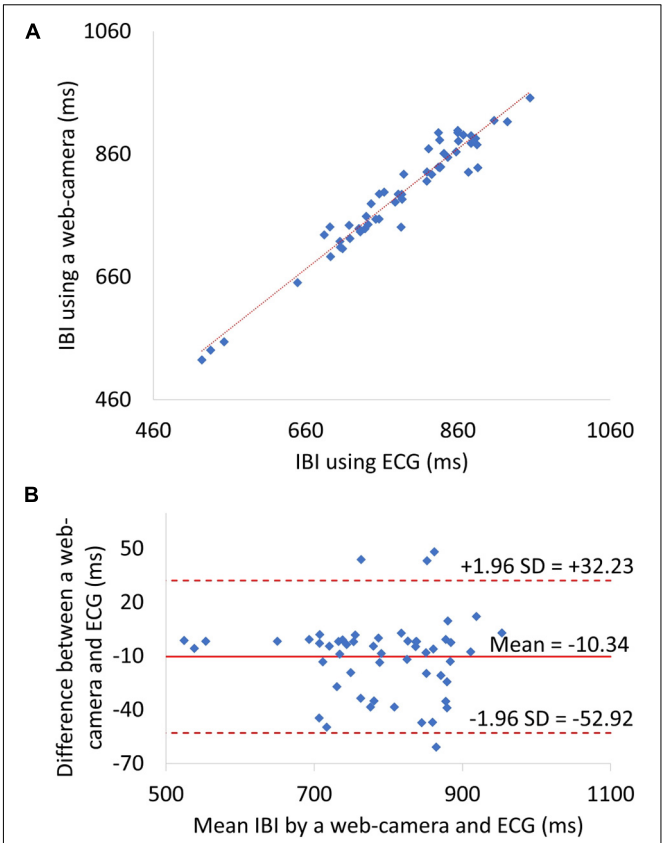

FIGURE 6 | (A) A Scatter plots showing relationship between web camera-determined IBI and ECG-derived interbeat interval (IBI). **(B)** IBI Bland–Altman plot. ECG, electrocardiogram; SD, standard deviation.

$LF_{(Pre-R)}$, $LF_{(MT)}$, $LF_{(Post-R)}$, $HF_{(Pre-R)}$, $HF_{(MT)}$, $HF_{(Post-R)}$, $LF/HF_{(Pre-R)}$, $LF/HF_{(MT)}$, and $LF/HF_{(Post-R)}$, their deviations between Pre-R and MT, and their deviations between MT and Post-R. Our previous study showed that MDD patients and healthy people showed different autonomic nervous responses induced by MT (Sun et al., 2016). As shown in **Figure 3**, the

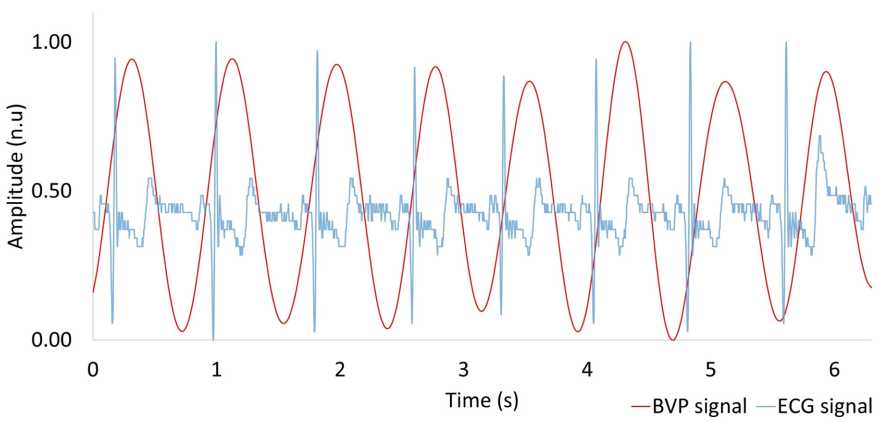

FIGURE 5 | Comparison between heartbeat signal measured by a web camera (red) and reference ECG (blue). BVP, blood volume pulse; ECG, electrocardiogram.

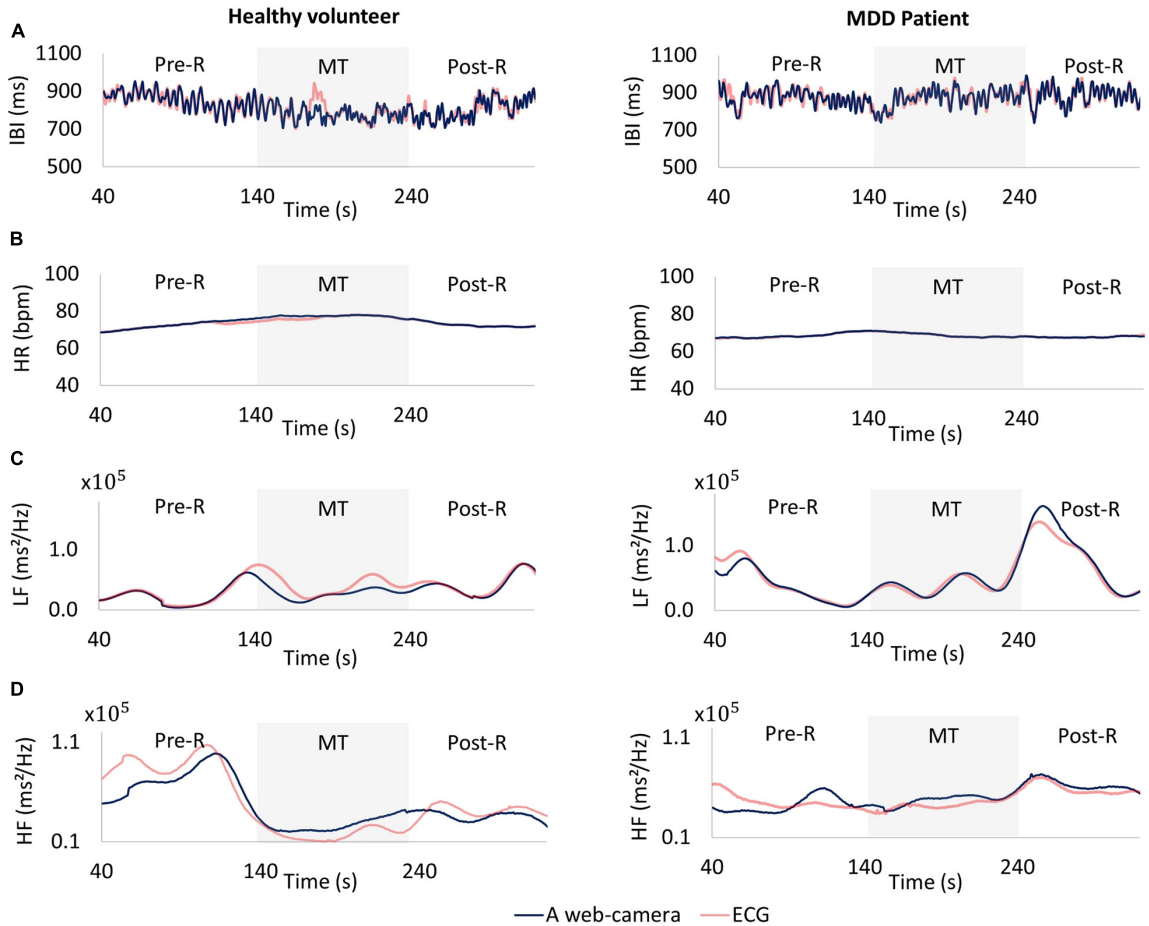

FIGURE 7 | Comparisons between a web camera-derived parameter (blue) and those determined by reference ECG (yellow). **(A)** Interbeat intervals (IBI), **(B)** heart rate (HR), **(C)** low frequency (LF), **(D)** and high frequency (HF) during the measurement. Left: A healthy volunteer, Right: A major depressive disorder (MDD) patient. The HF of a healthy volunteer reduced substantially during a stressful MT (**D** left), whereas that of an MDD patient showed no distinctive changes (**D** right). ECG, electrocardiogram; MT, mental task.

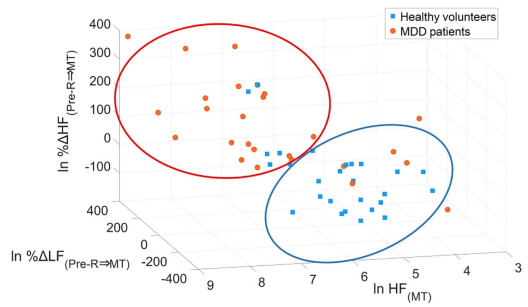

FIGURE 8 | Scatter plots of logarithmic expression illustrating the three explanatory variables of $HF_{(MT)}$, $\%\Delta LF_{(Pre-R\Rightarrow MT)}$, and $\%\Delta HF_{(Pre-R\Rightarrow MT)}$ in healthy volunteers and MDD patients. HF, high frequency; LF, low frequency; MDD, major depressive disorder; MT, mental task.

HF (corresponding to parasympathetic activity) of a healthy volunteer reduced substantially during MT, whereas the HF of an MDD patient showed no distinctive change during MT. To achieve an MDD screening accuracy equal to our previous study using ECG, we used the MRMR feature selection algorithm. This determined the optimal combination of LRA explanatory variables.

Evaluation and Setting of the System

Participants

A total of 26 MDD patients and 27 healthy volunteers were recruited. The patients (aged 20–58 years; 16 males and 10 females) were from the BESLI clinic, Tokyo, and all had a diagnosis of MDD according to the DSM-5 criteria and were not on antidepressant medication. The control participants (18–60 years; 15 males and 12 females) were volunteers from Tokyo Metropolitan University and RICOH Company, Ltd., who had never received a psychological disorder diagnosis. All participants were instructed not to consume alcohol and coffee for 24 h before the study and not to smoke tobacco on the day of the study. Zung (1965) Self-Rating Depression Scale (SDS) scores were used to evaluate the severity of symptomology for

all participants. An examinee with SDS cut-off score above 48 is suspected to having MDD (CIPS, 1996). SDS scores of all healthy volunteers in this study were below 48.

Regression analysis needs examinees ten times as many as the number of explanatory variables (Peduzzi et al., 1995). Our sample size of 53 examinees seems to be sufficient, while the number of explanatory variables is four. A chi-squared test revealed that there were no significant differences in the male/female ratio between MDD and healthy volunteer groups (p = 0.6). A chi-square test also revealed that there were no significant differences in age composition divided into three generations (a person younger than 25 years, a person aged 25 through 45 years, a person older than 45 years) in MDD and healthy volunteer groups (p = 0.2). A summary of the demographic of the healthy volunteers and the MDD patients is shown in **Table 1**.

This study was approved by the ethics committee of Tokyo Metropolitan University (approval number No 282) and BESLI clinic in Tokyo (approval number No 2018-001). All subjects provided written informed consent.

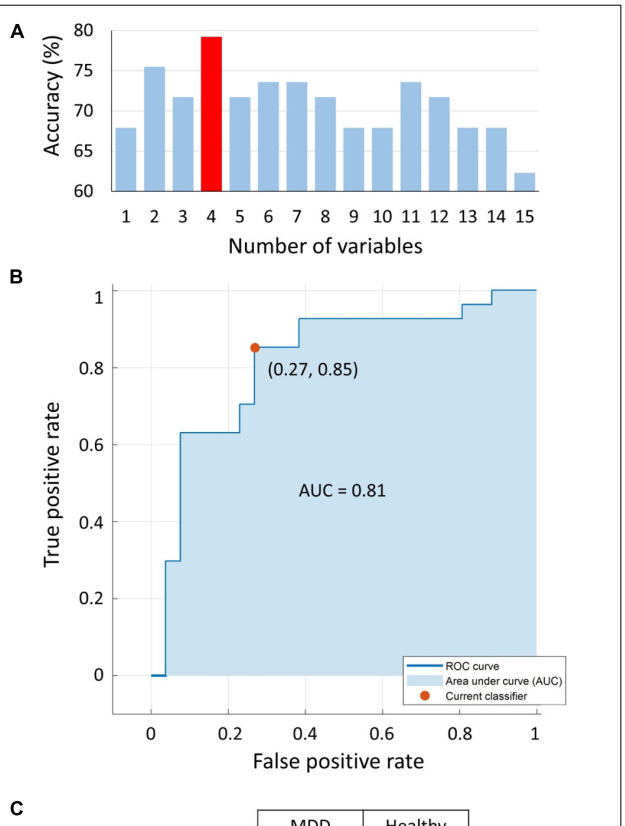

C

		MDD patients (n=26)	Healthy volunteers (n=27)	
Screening Result	MDD group	19	4	PPV 83%
	Healthy group	7	23	NPV 77%
		Sensitivity 73%	Specificity 85%	

FIGURE 9 | (A) Accuracy [mean of sensitivity, specificity, positive predictive value (PPV), and negative predictive value (NPV)] of logistic regression analysis (LRA) with 5-fold cross-validation as a function of number of explanatory variables; a combination of four explanatory variables exhibited the maximum accuracy. **(B)** The receiver operating characteristic (ROC) curve with area under the curve (AUC) of 0.81. **(C)** Confusion matrix of LRA corresponding to selected four explanatory variables to determine sensitivity, specificity, PPV, and NPV. MDD, major depressive disorder.

Study Protocol

The clinical tests were conducted indoors, and primary lighting was the only source of illumination in the room. Participants were seated on a chair in front of a 22-inch display (providing visual instructions) at a distance of approximately 60 cm during the test, as shown in **Figure 4**. The study protocol of the clinical test procedure contained three periods: pre-rest (Pre-R; 140 s), random number generation MT (MT; 100 s), and post-rest (Post-R; 120 s), with a total duration of 360 s. Participants executed the tasks by following visual and audio instructions. During the Pre-R and Post-R periods, participants were instructed to relax. During the MT, participants generated random numbers between 0 and 9. The frequency of the random number generation was regulated by a displayed instruction and a "beep" once per s. The facial RGB signal was captured by a web camera (LogiCool HD Pro C920, Logitech International S.A., Lausanne, Switzerland) at a frame rate of 30 frames/s, a color pixel resolution of 1920 × 1080, and 256 tones. I-lead ECG readings were acquired simultaneously from both wrists at a sampling rate of 100 Hz as a reference.

Statistical Analysis

Pearson's correlation coefficient and Bland–Altman plots were used for statistical analysis of the correlation between the web camera measurement and the reference. The MRMR algorithm was used to determine the optimal combination of explanatory variables for MDD classification. The results from the LRA classification model were used to calculate the sensitivity, specificity, negative predictive value (NPV), and positive predictive value (PPV). A 5-fold cross-validation was performed to evaluate the accuracy of the LRA. The receiver operating characteristic curve was calculated to set the optimal cutoff point of the LRA model. Student's t-test was conducted to statistically assess the logit scores of the LRA model.

RESULTS

Using the PPG technique described in section "Materials and Methods," we extracted the BVP signal from the web camera RGB green signal via MODWTMRA. The BVP signal and the reference I-lead ECG are shown in **Figure 5**. The BVP signal was synchronous with the cardiac cycle as determined by the I-lead ECG. The pulse transmission time (time delay from ECG R-wave to BVP peak) was approximately 120 ms.

The level of agreement between the web camera-based method and the reference ECG was assessed using the Pearson correlation coefficient (n = 53) and the Bland–Altman plot. Correlation scatter plots for IBI are shown in **Figure 6A**. The IBI determined

by the web camera significantly correlated with that calculated from the reference ECG (r = 0.97, $p < 0.0001$). The root mean squared error of IBI was 24.05. **Figure 6B** shows the Bland–Altman plot for IBI determined by web camera and ECG. The 95% limits of agreement of IBI measurements ranged from −52.92 to −10.34 ms (standard deviation σ = 21.72).

The web camera-derived IBI of an MDD patient changed in the same manner as that determined by reference ECG (**Figure 7A**, right), whereas the web camera-derived IBI of a healthy volunteer showed small differences from that determined by reference ECG (**Figure 7A**, left). The web camera-derived heart rate of a healthy volunteer and an MDD patient changed in the same manner as those determined by reference ECG (**Figure 7B**). The web camera-derived LF of an MDD patient changed in the same way as that determined by reference ECG (**Figure 7C**, right), whereas the web camera-derived IBI of an MDD patient showed small differences from that determined by reference ECG (**Figure 7C**, right). The HF of a healthy volunteer reduced substantially during a stressful MT (**Figure 7D**, left), whereas that of an MDD patient did not show any distinctive changes (**Figure 7D**, right). The web camera-derived HF of an MDD patient and a healthy volunteer changed in a similar, but not identical, way to that of the ECG-determined LF and HF.

Minimum redundancy maximum relevance determined the following optimal combination of four variables: $HF_{(MT)}(x_1)$, $\%\Delta LF_{(Pre-R\Rightarrow MT)}$ (x_2), $\%\Delta HF_{(Pre-R\Rightarrow MT)}$ (x_3), and $\%\Delta HF_{(MT\Rightarrow Post-R)}$ (x_4) from the 15 potential LRA explanatory variables described above. **Figure 8** shows the logarithmic expression of three explanatory variables: $HF_{(MT)}$, $\%\Delta LF_{(Pre-R\Rightarrow MT)}$, and $\%\Delta HF_{(Pre-R\Rightarrow MT)}$ from the four explanatory variables determined by the MRMR algorithm for MDD patients and healthy volunteers. The combination of these three explanatory variables effectively screened for MDD patients.

The MRMR algorithm determined the priority order of the previously mentioned 15 LRA explanatory variables. We used the combination of four high priority explanatory variables, as it showed the highest MDD screening accuracy (mean of sensitivity, specificity, PPV, and NPV, as shown in **Figure 9A**). The logit score (**Figure 10**; i.e., $\log\frac{p}{1-p}$) is expressed in the following equation using the optimal combination of four explanatory variables, where p is the probability and $\log\frac{p}{1-p}$ is the corresponding odds (Kessler and Bromet, 2013).

$$\begin{gathered} Logit\ Score = log\frac{p}{1-p} \\ = -1.2895 + 0.0013HF_{MT} + 0.0051\%\Delta LF_{(Pre-R\Rightarrow MT)} \\ -0.0001\%\Delta HF_{(Pre-R\Rightarrow MT)} - 0.0004\%\Delta HF_{(MT\Rightarrow Post-R)} \\ Logit\ Score \geqq 0 \Rightarrow Suspected\ of\ MDD \\ Logit\ Score < 0 \Rightarrow Healthy \end{gathered} \tag{2}$$

Receiver operating characteristic analysis was performed to determine the optimum cutoff point for the predicted logit scores of the LRA model to differentiate the two groups with an area under the curve of 0.81 (**Figure 9B**). The LRA confusion matrix with 5-fold cross-validation showed a sensitivity, specificity, NPV, and PPV of 73%, 85%, 77%, and 83%, respectively (**Figure 9C**).

The logit scores determined by equation (Kessler and Bromet, 2013) significantly correlated with SDS scores (r = 0.43, $p < 0.05$) (**Figure 10**).

DISCUSSION

To conduct MDD screening without risk of secondary exposure during the global COVID-19 pandemic, we developed a novel

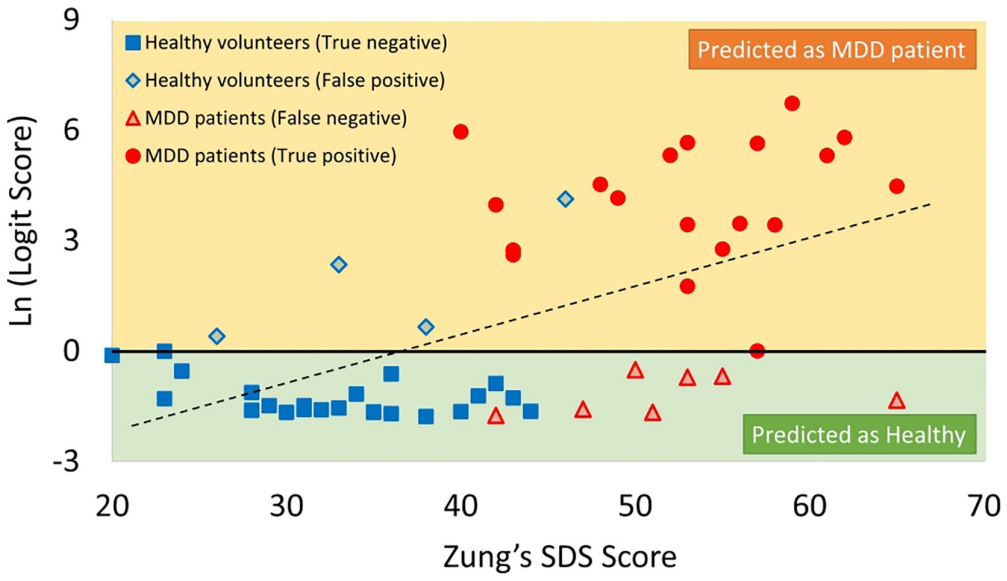

FIGURE 10 | Scatter plots of correlation between SDS score and logit score in logarithmic expression. MDD, major depressive disorder; SDS, Self-Rating Depression Scale.

web camera-based non-contact MDD screening system (WCF-MSS) based on autonomic nervous activity response induced by MT. The non-contact WCF-MSS achieved 73% sensitivity and 85% specificity.

To achieve high screening accuracy, we measured not only $HF_{(MT)}$, which reflects parasympathetic activation induced by MT, but also MT-induced percentage changes in HF and LF, which are related to sympathetic and parasympathetic nervous activities, using the variables $\%\Delta HF_{(Pre-R \Rightarrow MT)}$, $\%\Delta HF_{(MT \Rightarrow Post-R)}$, and $\%\Delta LF_{(Pre-R \Rightarrow MT)}$.

The WCF-MSS could be used not only with MDD patients but also with non-MDD high-risk groups, as the WCF-MSS logit score significantly correlated with SDS scores. Early-stage WCF-MSS-based MDD screening may enable effective and low-cost treatment (Andrews et al., 2004; Rush et al., 2006; Trivedi et al., 2006; Cuijpers et al., 2009). The WCF-MSS could be used to exclude malingering, as it enables screening without history taking.

Owing to the COVID-19 pandemic, the use of telemedicine in clinical psychiatry has become increasingly important. The Internet-connected WCF-MSS could be used as a telemedicine terminal. Web camera built-in smartphones, tablets, and laptop computers could be used with the WCF-MSS as telemedicine devices. The use of the WCF-MSS in telemedicine enables automatic pre-examination before history taking by a psychiatrist.

One of the study limitations was the small dataset (53 subjects) compared with typical datasets in the medical classification field. To address this limitation, future work based on the present study should include larger datasets to improve the accuracy of the LRA classifier. One potential problem with the WCF-MSS is the difficulty of excluding the effect of sudden large movements. Further improvements are required to reduce such system artifacts.

In summary, the MT-induced autonomic nervous response-based contact-free WCF-MSS with 5-fold cross-validation achieved 73% sensitivity and 85% specificity. WCF-MSS designed for home use may be useful as a preliminary inspection tool for potential MDD patients who hesitate to go to psychiatry hospitals. The WCF-MSS appears a promising contact-free MDD screening tool that can be used without spreading COVID-19 infection.

DATA AVAILABILITY STATEMENT

The raw data supporting the conclusion of this article will be made available by the authors, without undue reservation.

ETHICS STATEMENT

The studies involving human participants were reviewed and approved by The Ethics Committee of Tokyo Metropolitan University The Ethics Committee of BESLI clinic in Tokyo. The patients/participants provided their written informed consent to participate in this study. Written informed consent was obtained from the individual(s) for the publication of any potentially identifiable images or data included in this article.

AUTHOR CONTRIBUTIONS

BU and TM designed the research and wrote the manuscript. GS contributed to the writing of the manuscript. NT and FS supervised the medical aspects of MDD screening and performed clinical testing. GS, SW, MY, KF, FH, YY, and LC contributed to the image-processing and signal-processing methods. All authors reviewed the manuscript.

FUNDING

This study was funded by RICOH Company, Ltd. The funder was not involved in the study design; the collection, analysis, or interpretation of data; the writing of this article; or the decision to submit it for publication.

ACKNOWLEDGMENTS

We sincerely thank Saeko Nozawa for her contributions to manuscript preparation. This work was part of a research program with a project number NUM research grant (P2017-2506) supported by the National University of Mongolia. We are also grateful to all participants from BESLI clinic, RICOH Company, Ltd., and Tokyo Metropolitan University. We also thank Diane Williams, from Edanz Group (https://en-author-services.edanz.com/ac), for editing a draft of this manuscript.

REFERENCES

Andrews, G., Issakidis, C., Sanderson, K., Corry, J., and Lapsley, H. (2004). Utilizing survey data to inform public policy: comparison of the cost-effectiveness of treatment of ten mental disorders. *Br. J. Psychiatry* 184, 526–533. doi: 10.1192/bjp.184.6.526

Bassett, D. (2015). A literature review of heart rate variability in depressive and bipolar disorders. *Aust. New Zeal. J. Psychiatry* 50, 511–519. doi: 10.1177/0004867415622689

Bradski, G. (2000). The openCV library. *Dr. Dobbs J. Softw. Tools* 120, 122–125.

Brunoni, A. R., Kemp, A. H., Dantas, E. M., Goulart, A. C., Nunes, M. A., Boggio, P. S., et al. (2013). Heart rate variability is a trait marker of major depressive disorder: evidence from the sertraline vs. electric current therapy to treat depression clinical study. *Int. J. Neuropsychopharmacol.* 16, 1937–1949. doi: 10.1017/s1461145713000497

Carnevali, L., Thayer, J. F., Brosschot, J. F., and Ottaviani, C. (2018). Heart rate variability mediates the link between rumination and depressive symptoms: a longitudinal study. *Int. J. Psychophysiol.* 131, 131–138. doi: 10.1016/j.ijpsycho.2017.11.002

CIPS (1996). *Self-rating Depression Scale – German version*. Easton on the Hill: CIPS.

Cuijpers, P., Muñoz, R. F., Clarke, G. N., and Lewinsohn, P. M. (2009). Psychoeducational treatment and prevention of depression: the "coping with depression" course thirty years later. *Clin. Psychol. Rev.* 29, 449–458. doi: 10.1016/j.cpr.2009.04.005

Culpepper, L., Muskin, P. R., and Stahl, S. M. (2015). Major depressive disorder: understanding the significance of residual symptoms and balancing efficacy with tolerability. *Am. J. Med.* 128, S1–S15. doi: 10.1016/j.amjmed.2015.07.001

Dagdanpurev, S., Sun, G., Shinba, T., Kobayashi, M., Kariya, N., Choimaa, L., et al. (2018). Development and clinical application of a novel autonomic transient response-based screening system for major depressive disorder using a fingertip photoplethysmographic sensor. *Front. Bioeng. Biotechnol.* 6:64. doi: 10.3389/fbioe.2018.00064

Dockery, D. M., Rowe, S. G., Murphy, M. A., and Krzystolik, M. G. (2020). The ocular manifestations and transmission of COVID-19: recommendations for prevention. *J. Emerg. Med.* 59, 137–140. doi: 10.1016/j.jemermed.2020.04.060

James, S. L., Abate, D., Abate, K. H., Abay, S. M., Abbafati, C., Abbasi, N., et al. (2018). Global, regional, and national incidence, prevalence, and years lived with disability for 354 diseases and injuries for 195 countries and territories, 1990–2017: a systematic analysis for the Global Burden of disease study 2017. *Lancet* 392, 1789–1858. doi: 10.1016/s0140-6736(18)32279-7

Kalal, Z., Mikolajczyk, K., and Matas, J. (2010). "Forward-backward error: automatic detection of tracking failures," in *Proceedings of the 20th International Conference on Pattern Recognition*, Istanbul, doi: 10.1109/icpr.2010.675

Kessler, R. C., and Bromet, E. J. (2013). The epidemiology of depression across cultures. *Annu. Rev. Public Health* 34, 119–138. doi: 10.1146/annurev-publhealth-031912-114409

King, D. E. (2009). Dlib-ml: a machine learning toolkit. *J. Machine Learn. Res.* 10, 1755–1758.

Kwok, Y. L. A., Gralton, J., and Mclaws, M.-L. (2015). Face touching: a frequent habit that has implications for hand hygiene. *Am. J. Infect. Control* 43, 112–114. doi: 10.1016/j.ajic.2014.10.015

Lépine, J.-P., Gastpar, M., Mendlewicz, J., and Tylee, A. (1997). Depression in the community. *Int. Clin. Psychopharmacol.* 12, 19–30. doi: 10.1097/00004850-199701000-00003

Lewandowska, M., Ruminski, J., Kocejko, T., and Nowak, J. (2011). "Measuring pulse rate with a web-camera—a non-contact method for evaluating cardiac activity," in *Proceedings of the Federated Conference on Computer Science and Information Systems (FedCSIS)*, Szczecin.

Lienhart, R., and Maydt, J. (2002). "An extended set of Haar-like features for rapid object detection," in *Proceedings of the International Conference on Image Processing*, Rochester, NY, doi: 10.1109/icip.2002.1038171

Moser, M., Zapotoczky, G., Liebmann, P., Voica, M., Steinbrenner, B., Hildebrandt, G., et al. (1998). Increased heart rate in depressed subjects in spite of unchanged autonomic balance? *J. Affect. Disord.* 48, 115–124. doi: 10.1016/s0165-0327(97)00164-x

Peduzzi, P., Concato, J., Feinstein, A. R., and Holford, T. R. (1995). Importance of events per independent variable in proportional hazards regression analysis II. Accuracy and precision of regression estimates. *J. Clin. Epidemiol.* 48, 1503–1510. doi: 10.1016/0895-4356(95)00048-8

Poh, M.-Z., Mcduff, D. J., and Picard, R. W. (2011). Advancements in noncontact, multiparameter physiological measurements using a webcam. *IEEE Trans. Biomed. Eng.* 58, 7–11. doi: 10.1109/tbme.2010.2086456

Rush, A. J., Trivedi, M. H., Wisniewski, S. R., Nierenberg, A. A., Stewart, J. W., Warden, D., et al. (2006). Acute and longer-term outcomes in depressed outpatients requiring one or several treatment steps: a STAR*D report. *Am. J. Psychiatry* 163, 1905–1917. doi: 10.1176/ajp.2006.163.11.1905

Sun, G., Shinba, T., Kirimoto, T., and Matsui, T. (2016). An objective screening method for major depressive disorder using logistic regression analysis of heart rate variability data obtained in a mental task paradigm. *Front. Psychiatry* 7:180. doi: 10.3389/fpsyt.2016.00180

Suzuki, S., Matsui, T., Imuta, H., Uenoyama, M., Yura, H., Ishihara, M., et al. (2008). A novel autonomic activation measurement method for stress monitoring: non-contact measurement of heart rate variability using a compact microwave radar. *Med. Biol. Eng. Comput.* 46, 709–714. doi: 10.1007/s11517-007-0298-3

Trivedi, M. H., Rush, A. J., Wisniewski, S. R., Warden, D., Mckinney, W., Downing, M., et al. (2006). Factors associated with health-related quality of life among outpatients with major depressive disorder. *J. Clin. Psychiatry* 67, 185–195. doi: 10.4088/jcp.v67n0203

van Gent, P., Farah, H., van Nes, N., and van Arem, B. (2018). "Heart rate analysis for human factors: development and validation of an open source toolkit for noisy naturalistic heart rate data," in *Proceedings of the 6th HUMANIST Conference*, Hague, 173–178.

Viola, P., and Jones, M. J. (2004). Robust real-time face detection. *Int. J. Comput. Vis.* 57, 137–154. doi: 10.1023/b:visi.0000013087.49260.fb

von Arx, T., Tamura, K., Yukiya, O., and Lozanoff, S. (2018). The face – a vascular perspective. A literature review. *Swiss Dent. J.* 128, 382–392.

Vos, T., Allen, C., Arora, M., Barber, R. M., Bhutta, Z. A., Brown, A., et al. (2016). Global, regional, and national incidence, prevalence, and years lived with disability for 310 diseases and injuries, 1990–2015: a systematic analysis for the Global Burden of Disease Study 2015. *Lancet* 388, 1545–1602. doi: 10.1016/s0140-6736(16)31678-6

Wang, P. S., Aguilar-Gaxiola, S., Alonso, J., Angermeyer, M. C., Borges, G., Bromet, E. J., et al. (2007). Use of mental health services for anxiety, mood, and substance disorders in 17 countries in the WHO world mental health surveys. *Lancet* 370, 841–850. doi: 10.1016/s0140-6736(07)61414-7

Wang, W., Brinker, A. C. D., Stuijk, S., and Haan, G. D. (2017). Algorithmic principles of remote PPG. *IEEE Trans. Biomed. Eng.* 64, 1479–1491. doi: 10.1109/tbme.2016.2609282

Westen, D. (2012). Prototype diagnosis of psychiatric syndromes. *World Psychiatry* 11, 16–21. doi: 10.1016/j.wpsyc.2012.01.004

Whiteford, H. A., Degenhardt, L., Rehm, J., Baxter, A. J., Ferrari, A. J., Erskine, H. E., et al. (2013). Global burden of disease attributable to mental and substance use disorders: findings from the Global Burden of Disease Study 2010. *Lancet* 382, 1575–1586. doi: 10.1016/s0140-6736(13)61611-6

Woods, A. G., Iosifescu, D. V., and Darie, C. C. (2014). Biomarkers in major depressive disorder: the role of mass spectrometry. *Adv. Exp. Med. Biol. Adv. Mass Spectr. Biomed. Res.* 806, 545–560. doi: 10.1007/978-3-319-06068-2_27

Yan, H., Lu, S., Chen, L., Wang, Y., Liu, Q., Li, D., et al. (2020). Multiple organ injury on admission predicts in−hospital mortality in patients with COVID−19. *J. Med. Virol.* 93, 1652–1664. doi: 10.1002/jmv.26534

Yeragani, V. K., Pohl, R., Balon, R., Ramesh, C., Glitz, D., Jung, I., et al. (1991). Heart rate variability in patients with major depression. *Psychiatry Res.* 37, 35–46. doi: 10.1016/0165-1781(91)90104-w

Zung, W. W. K. (1965). A self-rating depression scale. *Arch. Gen. Psychiatry* 12:63. doi: 10.1001/archpsyc.1965.01720310065008

Conflict of Interest: SW was employed by the company Vital Lab, Ltd., and MY and KF were employed by the company RICOH Company, Ltd.

The remaining authors declare that the research was conducted in the absence of any commercial or financial relationships that could be construed as a potential conflict of interest.